ORIGINAL ARTICLE

The influence of microplastic and nanoparticles of environmental interest on the H_2O_2-KSCN-$CuSO_4$-NaOH oscillator-implications for ecotoxicology

Francois Gagne PhD, Chantale Andre MSc, Joelle Auclair MSc, Christian Gagnon PhD, Patrice Turcotte MSc

Gagné F, André C, Auclair J, et al. The influence of microplastic and nanoparticles of environmental interest on the H_2O_2-KSCN-$CuSO_4$-NaOH oscillator-implications for ecotoxicology. J Anal Toxicol Appl. 2018;2(1):1-6.

Background: In a context where emerging exotic chemicals of commercial interest are being produced by industry, understanding the fundamental properties of these compounds is important for environmental risk assessment.

Aim: We used the H_2O_2-KSCN-$CuSO_4$-NaOH oscillator in the presence of luminol to explore the effects of 5 nanoparticles ($nCeO_2$, nZnO, nCuZnFeO, nSmO and citrate-coated quantum dots) and a microplastic polyethylene bead on cyclic redox behavior in luminescence.

Methods: The oscillatory changes, indicators of contaminant interactions and associated regulation, were first examined in the presence of increasing concentrations of an antioxidant (electron donor), ascorbic acid, and an oxidant (electron acceptor), Ce(IV). The oscillator was then exposed to increasing concentrations of the 5 nanoparticles and microplastic beads for 15 min at room temperature and the resulting effects on the cyclic behavior of the oscillator were examined by Fourier transformation.

Results: In control conditions, the batch reaction produced 4 cyclic pulses of luminescence of 3.-6 min over a period of 15 min. Fourier transformation of the luminescence data revealed 2 major frequencies at 0.07 and 0.28, corresponding to periods of 14 and 3.6 min, respectively. The addition of the antioxidant ascorbic acid decreased the intensity of frequency 0.28, while the oxidant Ce(IV) produced luminescent changes at higher frequencies (0.43 and 0.5). It was observed that most of the tested compounds behaved like the oxidant Ce(IV), with the exception of citrate-coated quantum dots and CuZnFeO. A significant correlation was observed between the antioxidant potential (determined by the reduction of the phosphomolybdate complex) and the intensity of frequency 0.28 ($r=0.77$; $p<0.05$).

Conclusion: The appearance of signals at higher frequencies was also found in more complex biological systems, such as NADH changes in yeast cells exposed to oxidant compounds, which suggests that a chemical redox oscillator behaves similarly to a biochemical redox oscillator and can serve as a proxy to understand the influence of novel chemicals on redox oscillators.

Key Words: *Chemical oscillator; Redox potential; Environmental contaminant*

Oscillating reactions constitute a fascinating topic in chemistry with implications for biochemical and physiological phenomena. For instance, biochemical oscillations in metabolic energy precursors and gene expression were recognized for over 5 decades and are thought to be responsible for the circadian rhythm, which is constantly being observed in biology. From quorum sensing between bacteria (1,2), the production of redox intermediate during energy metabolism (3,4), cell division during embryogenesis and genetic clocks (2), oscillatory changes are commonly found in all forms of living organisms. Oscillations occur at the molecular level when at least 3 conditions are met: 1) the system is far from thermodynamic stability, 2) the reaction mechanism comprises at least one autocatalytic step and 3) the system possesses 2 steady states under initial conditions. One well-known chemical oscillator is the H_2O_2-KSCN-$CuSO_4$ oscillator in alkaline conditions developed by Orbán (5). This oscillator produces color changes or flashes of light in the presence of luminol and is also widely used in chemistry laboratories as an educational tool (6). The Orbán oscillator was the first example of a homogeneous liquid-phase, halogen-free system that oscillates in batch conditions. The detailed mechanism for cyclic light production is complex and is constructed from 2 non-autocatalytic mechanisms in alkaline conditions: H_2O_2-$CuSO_4$ and H_2O_2-KSCN (Figure 1). These mechanisms are coupled with various intermediates forming a feedback network which leads to oscillatory properties in light emission. In a closed system, luminescence peaks with periods ranging from 1-6 min are produced, depending on the relative concentrations and volume of the reagents. In this model, the formation and consumption of the yellow intermediate $HO_2Cu(I)$ is responsible for color oscillations. This intermediate also coincides with luminescence when luminol is added to the reaction medium (7). The species OS(O)CN-, which is generated from the radical OS(O)CN* (steps R1 to R4), provides a positive feedback loop. The negative feedback loop consists of the accumulation of HO* via steps R5 and R6 and consumes the autocatalytic intermediate OS(O)CN- in R7. The intermediate Cu+(SCN-)n reinitiates the positive feedback loop, which ends up as the products SO_4, HCO_3 and NH_4^+. Hence, the oscillation will eventually stop if the reagents are not replenished, as in the case of closed batch reactors.

Oscillators based on oxidative and reductive reactions could provide insight into the fundamental properties of new and exotic chemicals. They could also help to decipher the mechanisms by which oscillations in biochemical systems occur given that strong proton and electron flows in mitochondria during energy metabolism involve redox oscillations as well (8). The cyclic behavior of biochemical and genetic processes often show wave-like behaviors which ultimately form the basis of various cyclic and circadian rhythms in cells. Oscillators based on redox properties are of utmost interest given life had to adapt from an anaerobic to an aerobic environment during the Great Oxidation Event over 2.5 billion years ago (9). For example, the oxidation/reduction cycle of peroxiredoxin proteins was shown to follow the 24 h circadian cycle (cell time-keeping) from archaea to eukaryotes up to plants and mammals. From the environmental toxicology perspective, biomarkers, which are a measure of early biological effects of contaminants, often display non-linear periodic behavior, especially for those involved in redox homeostasis (10). The wave-like nature of biochemical responses is beginning to be acknowledged in ecotoxicology (11). The release of new and exotic compounds in the environment continues to raise concerns about their safety in the environment. Understanding the basic properties of emerging compounds such as microplastics and nanotechnology appeared of relevance to gain insight into their potential risk for the environment.

The purpose of this study was to examine the effects of 5 nanoparticles and polyethylene beads on luminescence oscillations. We used the H_2O_2-KSCN-$CuSO_4$-NaOH oscillator in the presence of luminol to examine the effects of xenobiotics on the frequency and intensity profiles of oscillation using Fourier transformation. The selected compounds were chosen based on their environmental interest, i.e., their potential to be found in the aquatic environment by municipal/industrial wastewaters. An attempt is made to discuss the observed changes in luminescence oscillations towards oscillations at the biochemical level in the context of toxicity effects.

Aquatic Contaminants Research Division, Environment and Climate Change Canada, Quebec, Canada

Correspondence: François Gagné, Aquatic Contaminants Research Division, Environment and Climate Change Canada, Quebec, Canada. Telephone 514 824 5379, e-mail francois.gagne@canada.ca

Received: January 29, 2018, Accepted: February 07, 2018, Published: February 14, 2018

MATERIALS AND METHODS

All reagents were purchased from Sigma-Aldrich chemical company (Ontario, Canada) at a purity of at least 98% or better. Cerium oxide ($nCeO_2$; <50 nm), samarium oxide (nSmO; <100 nm), zinc oxide (nZnO; <40 nm) and copper-zinc-iron (nCuZnFeO; <100 nm) nanoparticles were purchased from Materials Science (Sigma-Aldrich, Ontario, Canada). Citrate-coated cadmium tellurium green-emitting quantum dots were purchased from American Dye Source (USA). Microplastic polyethylene beads between 1-3 µm diameter were purchased at Cospheric (USA). They were all suspended in bidistilled water. Ascorbic acid and Ce(IV) oxide were obtained from Sigma-Aldrich (Ontario, Canada).

The oscillator model in this study is based on luminescence induced by the H_2O_2-KSCN-$CuSO_4$ reaction in alkaline condition developed by Orbán (5). Luminol was added to track the cyclic flow of electrons and could be sensitively measured by microplate luminescence. The reaction mixture (200 µL) was prepared in white 96-well microplates with the following concentrations: 25 mM NaOH, 1.5 mM $CuSO_4$, 3.75 mM KSCN, 250 mM H_2O_2 and 0.9 mM luminol. The test compounds were added at different concentrations in 50 µL volume to give the final concentrations of 0.04, 0.08 and 0.12 µg/ml for ascorbate; 1.7, 3.4 and 5 µg/ml for Ce(IV); 17, 34 and 50 µg/ml for polyethylene microplastic beads; 0.17, 0.34 and 1 mg/ml for $nCeO_2$; 0.17, 0.34 and 1 mg/ml quantum dots; 0.8, 1.6 and 2.5 mg/ml for nZnO; 4, 8 and 12 µg/ml for nCuZnFeO; and 80, 160 and 240 µg/ml for nSmO. The concentrations were selected to produce effects at the range of concentrations close to those used in the oscillator instead of searching for threshold effects. The compounds were diluted in bidistilled water and controls received only bidistilled water. The reaction was initiated with the addition of H_2O_2. Chemiluminescence was read in a microplate reader at bandpass filter for luminol photons (428 nm) (Synergy 4, Bioscan, USA) every 10-20 s for 15 min. The data were expressed as relative luminescence units.

The antioxidant properties of the above compounds were determined using the reduction of the phosphomolybdate complex methodology (12). Briefly, the tested substances were diluted to 1 mg/ml in bidistilled water. To 20 µL of tested sample, 180 µL of bidistilled water and 20 µL of phosphomolybdate complex (1 µg/ml in ethanol) were added. The reaction was incubated for 20 min at 20°C and absorbance was taken at 660 nm to measure the formation of the blue complex of reduced phosphomolybdate. Blank samples consisted of bidistilled water only. The data was expressed as the ratio of A660 sample/A660 blank.

DATA ANALYSIS

The exposure experiments were repeated 3 times. The luminescence data were then analyzed by spectral analysis using the Fourier transformation methodology. The analysis transformed the time-resolved data in luminescence into frequency-resolved data for luminescence. The Fourier transformation procedure models the periodic nature of the data by fitting sine and cosine functions at different frequencies. In essence, the procedure transforms any functions f(x,t) into functions of frequencies g(k). More precisely, the Fourier series is defined as:

$$g(k)=a0 + \Sigma[Ak* \cos (2\pi(kn/q)+Bk* \sin (2\pi(kn/q)]$$

Where, k=1 to q observations (time in the present case)

The coefficients n and q represent the individual and total observations respectively of the series expressed in time (min or h) or space (x) and k is the frequency. The constants Ak and Bk are used to calculate the periodogram (Pg) value, which is related to the amplitude variance of the sine and cosine functions at each frequency:

$$Pg=(Ak2 + Bk2) * q/2$$

The Pg value is thus related to the variance of the function at a given frequency. The relationships between the Pg values and phosphomolybdate reduction potential were examined using multiple regression analysis. Significance was set at $\alpha<0.05$.

RESULTS

The basic physico-chemical characteristics of the compounds in the present study are depicted in Table 1. We used ascorbic acid (antioxidant potential of 3.3) and Ce(IV) (antioxidant potential of 0.99) as the reducer (electron donor) and oxidant (electron scavenger) respectively. Cerium oxide and zinc oxide nanoparticles had the highest antioxidant potential with values of 1.6 and 1.2, respectively. Conversely, citrate-coated CdTe quantum dots, nCuZnFeO and polyethylene microplastic beads had the lowest reducing power with a redox potential close to that of Ce(IV). The Orbán oscillator was adapted to fit in 96-well microplates and in closed batch mode (Figure 2A). In these conditions, oscillatory changes lasted for 15 min with 3 large amplitudes in luminescence. Fourier transformation of the luminescence data (Figure 2B) revealed two major frequencies: 0.07 and 0.28, which corresponds to periods of 14 and 3.6 min. The reaction was examined with increasing amounts of a reducer (electron donor), ascorbate (Figure 3A). The frequency profiles revealed the loss in intensity at 0.28 frequencies with an increase in amplitude changes for the 0.07 frequency (Figure 3B). An initial increase in the luminescence signal was observed at frequency 0.07 for the first two ascorbate concentrations and followed by a drop at the highest ascorbate concentration. Regression analysis revealed that ascorbate concentration was not significantly related to frequency intensity at 0.07, but was negatively correlated (r=-0.99; p=0.01) with the next frequency intensity at 0.14. The reaction was examined in the presence of an electron acceptor (oxidant), Ce(IV) (Figure 4A). For the first 2 concentrations (1.7 and 3.4 mg/ml), the luminescent peaks are compressed in time while at the highest concentration (5 mg/ml), the shift was less pronounced. Frequency analysis revealed the appearance of higher frequencies at 0.43 to 0.5, which corresponds to a period of 2 min (Figure 4B). Regression analysis revealed that Ce(IV) concentrations were significantly correlated with the intensity of frequencies 0.43 (r=0.97; p=0.03) and 0.5 (r=0.95; p=0.05).

We examined the influence of polyethylene microplastic beads on luminescence oscillations. The presence of microplastic beads decreased the luminescence intensity and compressed somewhat the peaks in time (Figure 5). Indeed, frequency analysis revealed the loss of the frequency 0.28 with the appearance of signals at higher frequencies (0.43 and 0.5). Regression analysis revealed no significant changes in frequency intensity with microplastic concentrations. However, the frequency profile was similar to that of Ce(IV) based on hierarchical tree analysis, which suggests some capacity to capture electrons in these conditions (oxidant). The redox potential of the substances was also determined by the capacity to reduce the phosphomolybdate complex (Table 1). As expected, the redox potential of the microplastic beads was similar to that of Ce(IV), which indicates a low capacity to liberate electrons, i.e., devoid of antioxidant activity. The reduction potential was significantly correlated (r=0.77; p=0.001) with the intensity of frequency 0.28, which suggests the stronger the propensity to liberate electrons (antioxidant) in the system, the stronger the intensity of the at frequency 0.28, (3.6 min period). We also examined the influence of 5 different nanoparticles on luminescence changes (Figures 6A-6E). The tested nanoparticles were $nCeO_2$, nZnO, nCuZnFeO, CdTe quantum dots and nSmO. The Zeta potential and reduction potential of these nanoparticles are given in Table 1. The Zeta potential ranges from -45 mV for citrate-coated CdTe to +30 mV for nCeO. The reduction potential was determined by the capacity of the compounds to reduce the phosphomolybdate complex and revealed that microplastic beads, citrate-coated CdTe and nSmO had a very low reduction power compared with nCeO and nZnO, which had the highest value of 1.6 to 1.24 (ascorbate reduction value of 3.3). When nCeO was added to the reaction medium, 2 types of responses were observed. At low concentration of $nCeO_2$, a behavior close to ascorbate was observed with a decrease in the signal at 0.28 frequencies and an increase at 0.07 frequencies (Figure 6A). As the concentration increased, the decrease in the signal at 0.28 frequency was less severe with the appearance of signals at higher frequencies, as found with Ce(IV). Indeed, based on frequency responses, the $nCeO_2$ frequency profile was similar to those from Ce(IV) (Figure 7). A negative correlation with the exposure concentration and 0.21 (r=-0.97; p=0.02) and 0.28 frequencies (r=-0.98; p=0.01) was obtained. In the case of citrate-coated quantum dots, the luminescence profile was somewhat similar to that of ascorbic acid (Figure 6B) as the signal at frequency 0.28 was decreased. Regression analysis revealed the concentration was significantly correlated with frequency 0.07 (first frequency; r=0.95; p=0.05) and 0.14 (r=-0.95; p=0.05). In the case of nZnO, which displayed the highest reductive power, the luminescence spectra showed more intense peaks and the appearance of compressed peaks (Figure 6C). Frequency analysis revealed a chaotic pattern of signals at various frequencies, at the expense of the characteristic signal at frequency 0.28. Regression analysis revealed that the exposure concentration was not related to the intensity of any frequencies.

The addition of increasing concentrations of CuZnFeO nanoparticles in the reaction media decreased the luminescent intensity at the highest concentration (12 µg/ml) (Figure 6D). The formation of 4 luminescent peaks was observed compared with the 3 peaks of the controls. Based on the frequency profiles, CuZnFeO nanoparticles were closely associated with neither the electron donor ascorbate nor the electron acceptor

$2\ H_2O_2 + SCN^- \rightarrow OS(O)CN^- + 2\ H_2O$ (R1)

$2\ OS(O)CN^- \rightarrow OOS(O)CN^- + OSCN^-$ (R2)

$H_2O + OS(O)CN^- + OOS(O)CN^- \rightarrow 2\ OS(O)CN\bullet + 2\ OH^-$ (R3)

$OS(O)CN\bullet + Cu^+\{SCN^-\}n \rightarrow OS(O)CN^- + Cu^{2+} + n\ SCN^-$ (R4)

$H_2O_2 + Cu^{2+} + OH^- \rightarrow HO_2Cu(I) + H_2O$ (R5)

$HO_2Cu(I) + n\ SCN^- \rightarrow Cu^+\{SCN^-\}n + HO^\bullet_2$ (R6)

$OS(O)CN^- + HO^\bullet_2\ SO3^{2-} + HOCN$ (R7)

Figure 1) *Key steps for oscillatory behavior of the H_2O_2-KSCN-Cu(II) oscillator (5)*

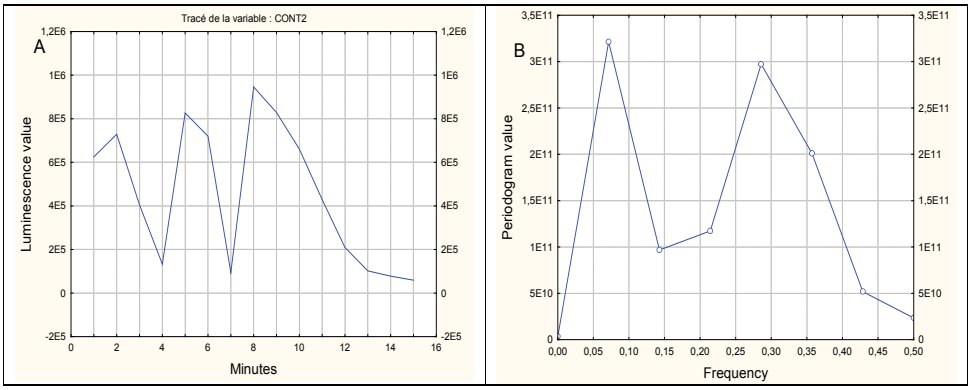

Figure 2) *Cyclic changes in luminescence over time*

The reaction was allowed to proceed in a 96-well microplate for 15 min. Luminescence data and corresponding frequency analysis are shown in A and B, respectively

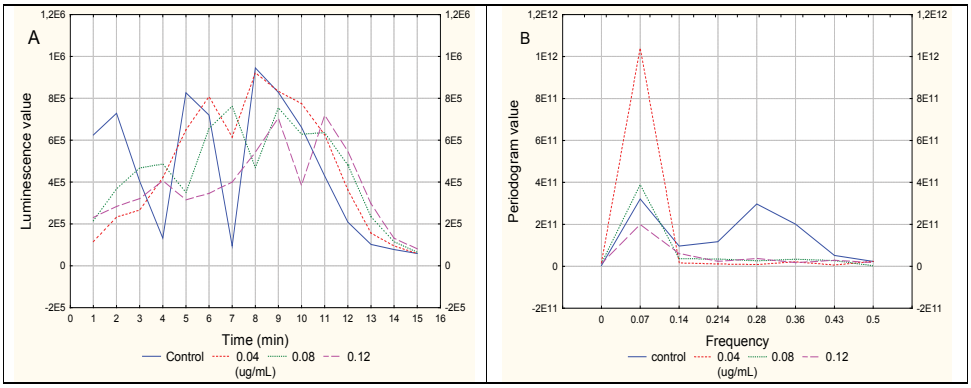

Figure 3) *Oscillator behavior in the presence of a reducer (electron donor)*

The Orbán oscillator reaction was examined in the presence of increasing amounts of ascorbate. The changes in luminescence (A) and frequency analysis (B) are shown

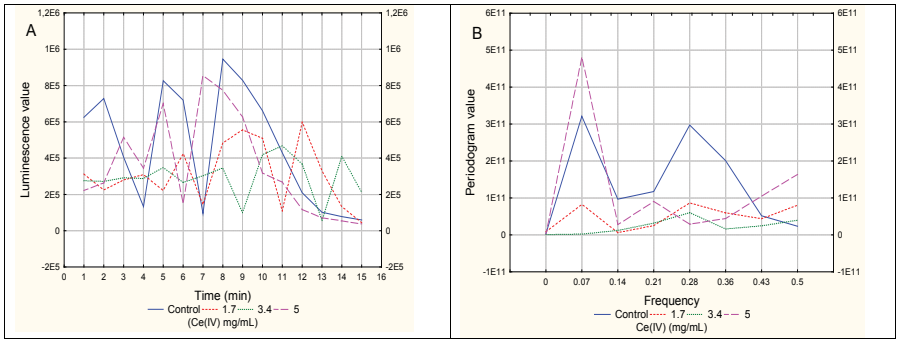

Figure 4) *Oscillator behavior in the presence of an electron acceptor*

The Orbán oscillator reaction was examined in the presence of increasing amounts of ascorbate. The changes in luminescence (A) and frequency analysis (B) are shown

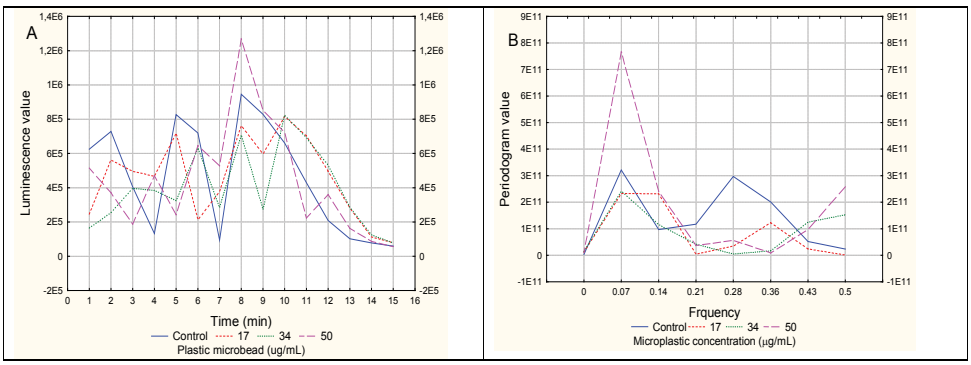

Figure 5) *Oscillation changes in the presence of polyethylene microplastic beads*

The reaction mixture was mixed with increasing concentrations of polyethylene microbead (1-3 µm). The changes in luminescence (A) and frequency analysis (B) are shown

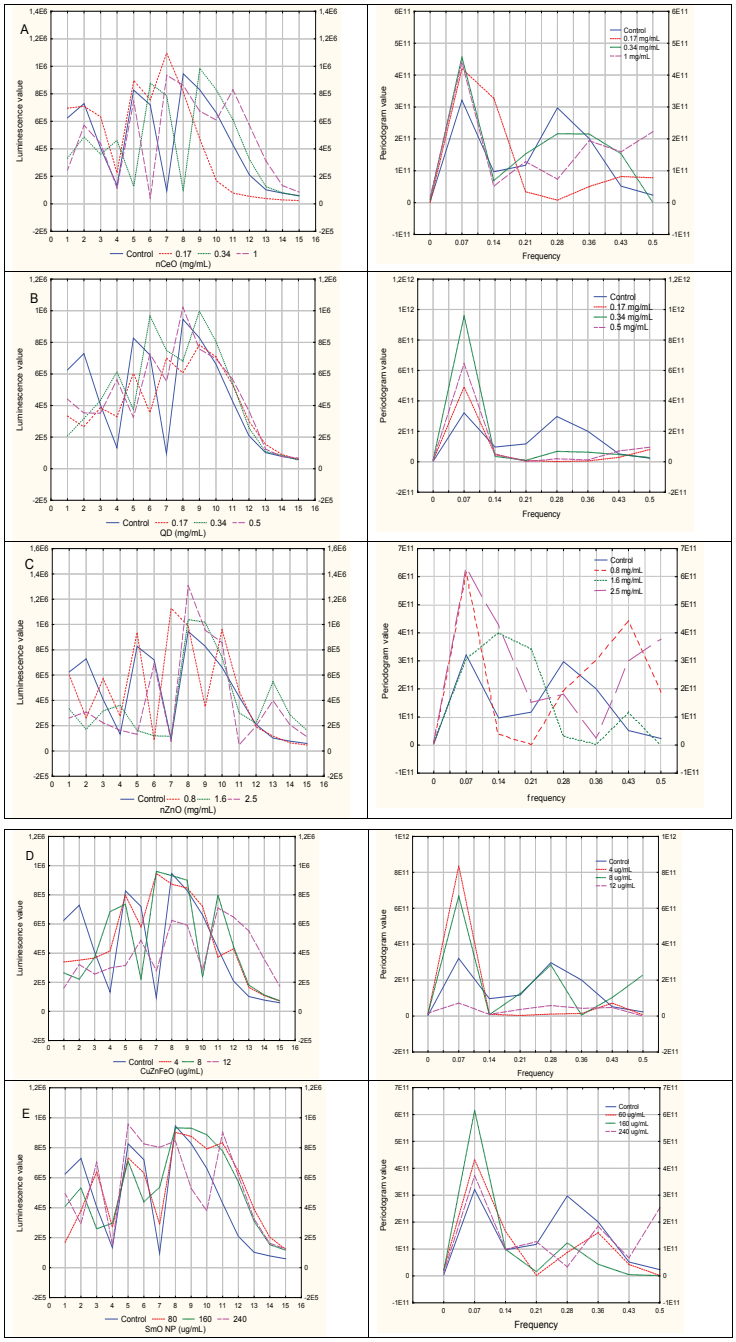

Figure 6) *Oscillation changes with selected nanoparticles*

The influence of 5 nanoparticles was examined in the Orbán reaction. The luminescence data for $nCeO_2$, CdTe (B), ZnO (C), CuZnO (D) and SmO (E) are shown. The frequency profiles obtained after Fourier transformation appear on the right side of each figure

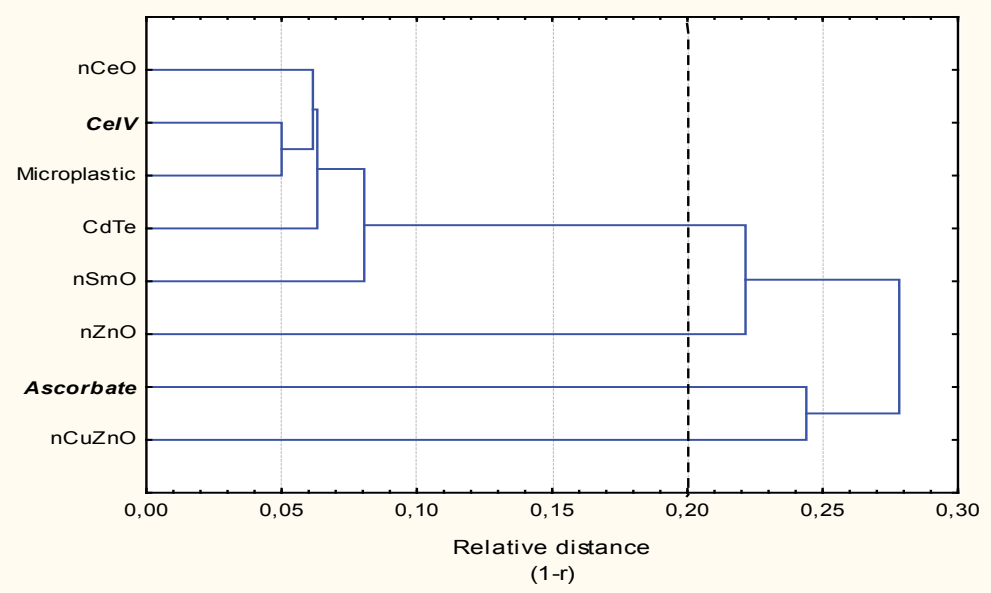

Figure 7) *Hierarchical tree analysis of changes in frequency for the selected compounds*

The first 8 frequencies were used to seek a common pattern between the frequencies. The dotted line represents the significance limit ($p<0.05$ for $(1-r)$ values <0.2) for the correlation values (r)

TABLE 1

Physical-chemical characteristics of the tested substances

Compounds	Provider/ Distributer	Properties			
		MW [1]	Size	Zeta potential (mV)	Reduction potential[2]
$nCeO_2$	Sigma-Aldrich (Canada)	172 (CeO_2)	<50 nm	+30	1.6
nZnO	Sigma-Aldrich (Canada)	82 (ZnO)	<40 nm	+24	1.24
CdTe-citrate coated	ADS American Dye Source (USA)	240 (CdTe)	4 nm (green emitting)	-45	1.02
nSmO	Sigma-Aldrich (Canada)	347 (Sm_2O_3)	<100 nm	+23	1.18
nCuZnFeO	Sigma-Aldrich (Canada)	144 (CuZFeO)	<100 nm	--	0.9
Microplastic polyethylene beads	Cospheric (USA)	--	1-3 µm	--	1.01
Ascorbate	Sigma-Aldrich (Canada)	198 (Na salt)	<1 nm	--	3.3
Ce(IV)	Sigma-Aldrich (Canada)	332 (2 × SO_4 salt)	<1 nm	--	0.99

[1]Molecular weight of molecular species in parentheses in g/mol; [2]The reduction potential was determined by phosphomolybdate reduction assay (A660 nm) at 1 mg/ml concentration

Ce(IV). Moreover, no significant relations were found between exposure concentrations and the intensity of each 8 frequencies. The influence of SmO nanoparticle concentration on the oscillations was also examined (Figure 6E). The intensity of the luminescent peaks was not overly affected by nSmO but produced a 4th luminescent peak which was not present in the controls (the peak at 12 min). Frequency analysis by Fourier transformation revealed a decrease in intensity of frequency 0.28, with a shift at frequency 0.36 and 0.5 suggesting the appearance of higher frequencies. Based on the frequency profiles (Figure 7), the behavior of nSmO was similar to that of the electron acceptor Ce(IV). There was no significant correlation between exposure concentration and the signal intensity for each frequency.

DISCUSSION

The batch reaction of the H_2O_2-KSCN-$CuSO_4$-NaOH oscillator allows for continuous oscillations up to 15 min in this closed system with periods of between 3-4 min. This is similar to the global time of 12 min observed in previous studies with the appearance of peaks at 1.5-2 min intervals (13). Frequency analysis by Fourier transformation revealed 2 main frequencies in the luminescence profiles: 0.07 and 0.28. The light emissions at the 0.28 frequency (period of 3.6 min) are associated with the main reaction, which involved the formation of copper hydroperoxide: $HO_2Cu(I)$. Indeed, a narrow burst of light with an intensity proportional to the concentration of luminol occurred at the same time as the formation of this copper peroxide complex $HO_2Cu(I)$ (14). A second set of broad low-intensity oscillations is apparent when luminol concentrations are <0.1 mM, which are associated with the slower reaction of luminol with superoxide anion. This is perhaps related to the signal with a large period at the 0.07-0.14 frequencies. In another study using thiocarbamide instead of luminol as the luminescent reagent, decreasing copper concentrations down from 0.1 to 0.01 mM decreased the number of luminescent peaks (lower frequency) with no apparent influence on the amplitudes (7). The same influence for Cu(II) concentrations was also observed with concentrations <0.5 mM $CuSO_4$ with luminol as the luminescent reagent (13). Exposure to the antioxidant ascorbic acid reduced the frequency of luminescence change, which suggests that ascorbic acid has an effect similar to decreasing Cu(II) or luminol concentrations. Indeed, ascorbic acid could compete with luminol, which requires an oxidant to produce luminescence. In addition, ascorbic acid could reduce Cu(II) to Cu(I) with the formation of an ascorbate radical, which could increase the baseline luminescence profiles resulting in smaller amplitude changes in luminescence (Figure 3A). This would tend to dampen the cyclic oscillation in luminescence at the expense of increasing the baseline luminescence. This was also observed with citrate-coated CdTe quantum dots where a decrease in luminescence frequency (at 0.28) and increase in baseline luminescence were observed. This was less apparent with CuZnFeO nanoparticles, suggesting electron donor (reductant) properties which have an equivalent effect of decreasing Cu(II) effective concentration in the reaction medium. Compounds capable of chelating Cu(II) could produce important effects on oscillations in luminescence (14). The addition of EDTA would increase both luminescence and the period (lower frequency), while the addition of thiols such as cysteine and methionine would decrease the amplitude with increased time between luminescence peaks (lower frequency). The addition of non-

ionic and ionic surfactants increased the intensity of oscillating luminescent reaction by up to 5 times (14). However, large increases in amplitude were not observed near the normal frequency (0.28) with the tested compounds in the present study, with the exception of increases at the low frequency signal (0.07-0.14) with some of the compounds, including citrate-coated quantum dots, nZnO, microplastic polyethylene beads and nCuZnFeO.

In the other cases, i.e., with microplastic polyethylene beads, $nCeO_2$, nZnO and nSmO, the appearance of luminescence at higher frequencies was observed. In most cases, amplitudes were increased for these compounds with the exception of nSmO. The behavior was similar to the electron acceptor/scavenger Ce(IV), which produced changes at higher frequencies but with increased amplitude changes. Citric acid, triethyletetramine and penicillamine (oxygen and amine-based chelators) increased the frequency in luminescence as well, but not the amplitudes (14). This suggests that these compounds contain electrophilic sites. Some increase in amplitudes at higher frequencies was observed for citrate-coated quantum dots, but the electron donor (reductive) behavior was more apparent, i.e., loss of the signal at frequency 0.28 with increases in amplitudes at frequency 0.07. The concentrations of KSCN and H_2O_2 were shown to influence the period (frequency) of oscillations (13). The concentration of H_2O_2 was directly proportional to the frequency and intensity of luminescence, while the concentration of KSCN was indirectly proportional to the frequency and intensity of luminescence signals. KSCN is involved in the stabilization of Cu^{1+} either directly (SCN) or indirectly following oxidation by H_2O_2 (SO_2CN^-) at step R1 (Figure 1). This is consistent with the significant correlation between the redox potential and the intensity of frequency 0.28 ($r=0.77$; $p=0.04$). This suggests that electron acceptor molecules such as Ce(IV) and those above tend to stabilize -SCN perhaps by Ce(IV) + K^+ + SCN^- Ce(III)SCN + KOH (in alkaline condition) and facilitate (catalysis) electron transfer of H_2O_2 to Cu perhaps through Ce(IV) and Ce(III) redox reactions. The standard reduction potential for Ce(IV) to Ce(III) is 1.44 V, just below the reduction potential of H_2O_2 to H_2O + 2e + $2H^+$ of 1.763 V, which is consistent for such a coupling in the luminescent oscillator. These potential values are one order of magnitude stronger than the reduction potential for Cu(II) to Cu(I) of 0.159 V. Increasing luminol concentrations from 2.4 mM to 120 mM decreased the number of luminescence peaks, but at a higher intensity (13,15). In the present study, the luminol concentration was below the concentrations used at 1 mM, which resulted in 3 to 4 major luminescent peaks with a maximum emission 4.5 times the baseline luminescence.

Understanding the fundamental properties of oscillators, which involve coupled redox reactions, could provide some insight into how biochemical oscillations behave independently of genetic regulation. The cyclic changes in the peroxiredoxin oxidation state were shown to follow 24 h circadian rhythms in all aerobe organisms (9). This process is independent of gene expression given that redox 24 h cycles of peroxiredoxins were observed in red blood cells *in vitro* (16,17). These oscillations persist for many days without the need of any external cues. Transcription is not required for circadian oscillations indicating that more basic non-transcriptional events seem to be enough for sustained cellular circadian rhythms. It is possible that the underlying metabolic redox activity (anaerobic and aerobic respiration, glycolysis) could induce changes at the biochemical level before reaching the level of protein and cellular signaling. For example, the oxidation–reduction cycles of peroxiredoxin proteins constitute a universal marker of circadian rhythms in all domains of life (i.e., from archea to eukaryotes) where redox homeostatic mechanisms are coupled with cellular time-keeping mechanisms in organisms following the Great Oxidation Event over 2.5 billion years ago (9). Many of the examined nanoparticles behaved as oxidants (electron scavengers) in the present study and led to the formation of low amplitudes in luminescence at higher frequencies. This phenomenon was also observed in the cyclic changes in the electron donor NADH in yeast cell suspensions supplemented with glucose (18). Exposing yeast cells to Cu(II), silver nanoparticles and Gd(III) for 3 h led to the formation of higher frequencies with concentration-dependent amplitude changes. This suggests that these electron acceptor molecules were also able to produce changes at higher frequency for NADH levels during glycolysis. In another study in mussels placed in toxic aeration lagoons treating municipal wastewaters, the appearance of cyclic changes at higher frequencies in biomarkers involved in redox equilibrium/maintenance were also observed (18). Indeed, metallothioneins, lipid peroxidation and peroxidase activity were changed at frequencies and amplitudes higher than those observed in mussels placed in natural water. Moreover, phase analysis revealed that these frequencies were not displaced with those of the reference mussels, which suggests heterogeneous responses or the appearance of toxicity-related frequencies that seemingly were absent in control mussels. More research will be needed to explore the relationships between chemical oscillations that normally occur during life processes and whether the frequency of these changes could be modulated and resonate at higher levels of biological organization. In this respect, the examination of the interaction of chemicals with "simple" chemical oscillators could provide insights into the many fundamental life processes that follow wave-like behavior.

CONCLUSION

The appearance of signals at higher frequencies was also found in more complex biological systems, such as NADH changes in yeast cells exposed to oxidant compounds, which suggests that a chemical redox oscillator behaves similarly to a biochemical redox oscillator and can serve as a proxy to understand the influence of novel chemicals on redox oscillators.

ACKNOWLEDGEMENT

This work was funded by the Chemical Management Plan (Nanotechnology) of Environment and Climate Change Canada.

REFERENCES

1. Delfino Perez P, Hagen SJ. Heterogeneous response to a quorum-sensing signal in the luminescence of individual *Vibrio fischeri*. PLoS One. 2010;5:e15473-81.
2. Danino T, Mondragon-Palomino O, Tsimring L, et al. A synchronized quorum of genetic clocks. Nature. 2010;463:326-30.
3. Pye K, Chance B. Sustained sinusoidal oscillations of reduced pyridine nucleotide in a cell-free extract of *Saccharomyces carlsbergensis*. Proc Natl Acad Sci U S A. 1966;55:888-94.
4. MacDonald MJ, Fahien LA, Buss JD, et al. Citrate oscillates in liver and pancreatic Beta cell mitochondria and in INS-1 insulinoma cells. J Biol Chem. 2003;278:51894-900.
5. Orbán M. Oscillations and bistability in the copper(II)-catalyzed reaction between hydrogen peroxide and potassium thiocyanate. J Am Chem Soc. 1986;108:6893-8.
6. Prypsztejn HE. Chemiluminescent oscillating demonstrations: The chemical buoy, the lighting wave and the ghostly cylinder. J Chem Educ. 2005;82:53-4.
7. Sorouraddin MH, Iranifam M. Oscillating chemiluminescence with thiosemicarbazide in a batch reactor. Luminescence. 2008;23:303-8.
8. Aon MA, Cortassa S, O'Rourke B. Mitochondrial oscillations in physiology and pathophysiology. Adv Exp Med Biol. 2008;641:98-117.
9. Edgar RS, Green EW, Zhao Y, et al. Peroxiredoxins are conserved markers of circadian rhythms. Nature. 2012;485:459-64.
10. André C, Gagné F. Effect of the periodic properties of toxic stress on the oscillatory behaviour of glycolysis in yeast-evidence of a toxic effect frequency. Comp Biochem Physiol. 2017;196:36-43.
11. Gagné F. The wave nature of molecular responses in ecotoxicology. Curr Top Toxicol. 2016;12:11-24.
12. Stanton MG. Colorimetric determination of inorganic phosphate in the presence of biological material and adenosine triphosphate. Anal Biochem. 1968;22:27-34.
13. Samadi-Maybodi A, Ourad SM. Studies of visible oscillating chemiluminescence with a luminol-H_2O_2-KSCN-$CuSO_4$-NaOH system in batch reactor. Luminescence. 2003;18:42-8.
14. Sorouraddin MH, Iranifam M, Amini K. A new enhanced oscillating chemiluminescence system with increased chemiluminescence intensity and oscillation time. J Fluoresc. 2008;18:443-51.
15. Sattar S, Epstein IR. Interaction of luminol with the oscillating system H_2O_2-KSCN-$CuSO_4$-NaOH. J Phys Chem. 1990;94:275-7.
16. O'Neil JS, Reddy AB. Circadian clocks in human red blood cells. Nature. 2011;469:498-507.
17. Hendriks GJ, Gaidatzis D, Aeschimann F, et al. Extensive oscillatory gene expression during *C. elegans* larval development. Mol Cell. 2014;53:380-92.
18. Gagné F, André C. Fourier transformation analysis of stress biomarkers in mussels exposed to lethal municipal effluents. Biomarker Appl. 2017;102:1-8.